Modeling of Flicker Noise in Quasi-ballistic FETs

Avirup Dasgupta and Yogesh Singh Chauhan
Department of Electrical Engineering, Indian Institute of Technology Kanpur, India
Email: avirup@iitk.ac.in, chauhan@iitk.ac.in

***Abstract*—In this paper we present a model for the Flicker noise in quasi-ballistic transistors based on our improved core transport model. The model is validated with DC and noise measurements for an $InGaAs$ nanowire FET and a Carbon nano-tube FET. The noise model, along with the core is valid from drift-diffusive to quasi-ballistic regimes of operation.**

***Index Terms*—Quasi-ballistic, Nanowire, CNT, InGaAs, Noise, Flicker noise, Compact Model, SPICE**

I. Introduction

Continuous scaling of Field Effect Transistors (FETs) has resulted in channel lengths of the order of the mean free path for electron flow. The drift-diffusive transport mechanism of long channel transistors is dictated by continuous scattering of all electrons resulting in lateral field dependent velocities. However, with continued scaling, this has now given way to the quasi-ballistic transport, where different electrons scatter to different degrees and some might even flow without scattering [1–14]. This change in the transport mechanism affects the distribution of the potential drop and the carrier concentration in the channel, which in turn affects the device behaviour. As expected, apart from the terminal current-voltage (I-V) characteristics, this shift in transport mechanism also changes the noise behaviour observed in such devices [15], [16].

Since the scattering events are random, it is difficult to analytically model a quasi-ballistic device, especially for SPICE simuations where computational efficiency is of high priority. Existing models use empirical formulations for channel potential [3], [5], [6], channel charge [7], transmission coefficient [8], effective velocity [9] and effective mobility [10]. Some also use sub-circuit based approach [11], [12] or rely on smoothing functions to stitch separate models for linear and saturation regions [13]. However, none of these include a model for the noise behaviour.

We have already presented a model for quasi-ballistic devices based on a simple scattering picture [2], [17]; along with the only existing model for flicker noise for such devices [16]. Here we present a new model for flicker noise based on the improved core model for quasi-ballistic FETs [17].

II. Transport model

Assuming a parabolic potential profile perpendicular to the channel and with suitable boundary conditions, the 2D Poisson equation in the channel can be reduced to a 1D equation given as [2], [17]

$$\frac{1}{\kappa}\frac{\partial^2\psi_c}{\partial x^2}+\frac{V_{gfb}-\psi_c}{\xi}=\frac{q}{\epsilon_s}n(x) \tag{1}$$

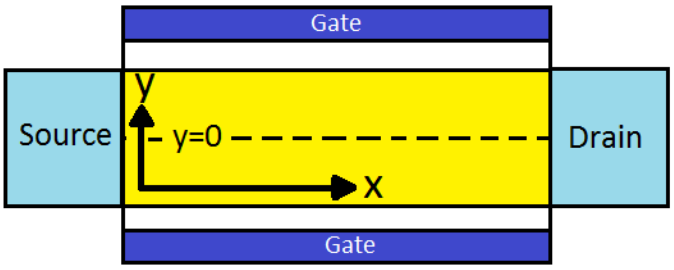

Fig. 1: A graphical representation of the cross-section of a generic FET showing the choice of axes.

where x is the transport direction as shown in Fig. 1, q is the electronic charge, $V_{gfb}=V_g-V_{fb}$ with V_g denoting the gate voltage and V_{fb} denoting the flat-band voltage; ψ_c denotes the center potential, $n(x)$ denotes the carrier concentration, $\kappa=1+\frac{\epsilon_{ins}T_s}{\epsilon_s T_{ins}}$ and $\xi=\frac{\epsilon_s T_{ins}T_s\kappa}{\epsilon_{ins}}$. T_s represents the semiconductor thickness while ϵ_{ins} and ϵ_s denote the permittivities of the insulator and the semiconductor respectively.

The condition for current continuity is given as [17]

$$\underbrace{n_b v_b}_{Ballistic}+\underbrace{\mu n_{dd}\frac{\partial\psi_c}{\partial x}}_{Drift}+\underbrace{\mu\phi_t\frac{\partial n_{dd}}{\partial x}}_{Diffusion}=constant \tag{2}$$

where n_b is the ballistic carrier density, v_b is the ballistic velocity and n_{dd} is the drift-diffusive carrier density [17]. μ denotes the mobility and ϕ_t denotes the thermal voltage. The Poisson equation along the channel coupled with the requirement for current conservation at every point along the channel gives [17]

$$\mu\frac{\partial n_{dd}}{\partial x}\frac{\partial\psi_c}{\partial x}+\mu n_{dd}\frac{\partial^2\psi_c}{\partial x^2}+\mu\phi_t\frac{\partial^2 n_{dd}}{\partial x^2}=0 \tag{3}$$

In our previous work [17] we have shown that the carrier density along the channel for the charges flowing from the source to the drain can be given as [17]

$$\begin{aligned} n_{dd-source}(x)&=n_s\frac{S}{1-S}\gamma^{(x/\lambda)}=n_{0s}\gamma^{(x/\lambda)};\\ n_{b-source}&=(1-S)^{L/\lambda}n_s \end{aligned} \tag{4}$$

where $n_{dd-source}$ and $n_{b-source}$ represent the drift-diffusive component and the ballistic component, respectively. Also, $n_{0s}=n_s\frac{S}{1-S}$ and γ is a material dependent parameter, with n_s denoting the source-side carrier density. From [2], $\gamma=(1-S)$, where S is the fraction of incoming charge carriers that scatter at every λ interval. Similarly the drift-diffusive and ballistic

$$\psi = \frac{e^{\frac{-\kappa}{\alpha\xi}x}}{\kappa}\left[\frac{\alpha\xi M_1 e^{\frac{\kappa}{\alpha\xi}x}}{\kappa} - \frac{N_1\gamma^{x/\lambda}e^{\frac{\kappa}{\alpha\xi}x}}{\alpha+\frac{\kappa}{\alpha\xi}} + C_1\right] + \frac{e^{\frac{\kappa}{\alpha\xi}x}}{\kappa}\left[\frac{-\alpha\xi M_2 e^{-\frac{\kappa}{\alpha\xi}x}}{\kappa} - \frac{N_2\gamma^{-x/\lambda}e^{-\frac{\kappa}{\alpha\xi}x}}{\alpha+\frac{\kappa}{\alpha\xi}} + C_2\right] + (\kappa-1)V_{gfb} \quad (6)$$

$$I_b = qT_sW\left(n_{b-source}v_b(x=0) - n_{b-drain}v_b(x=L)\right)\left[\frac{1-e^{-A\cdot V_{ds}/\phi_t}}{1+e^{-A\cdot V_{ds}/\phi_t}}\right] \quad (8)$$

$$I_{dd} = \frac{q\mu WT_s}{L}\Big[\left(\frac{N_2n_{0s}+N_1n_{0d}}{\alpha+\kappa'}\right)\alpha L - \frac{N_1n_{0s}}{2(\alpha+\kappa')}\left(\gamma^{-2L/\lambda}-1\right) + \kappa' n_{0s}\left(\kappa'+\alpha^{-1}\right)\left\{\gamma^{L/\lambda}\left(C_1e^{-\kappa' L}+C_2e^{\kappa' L}\right)-(C_1+C_2)\right\} \quad (9)$$

$$-\kappa' n_{0d}\left(\kappa'+\alpha^{-1}\right)\left\{\gamma^{-L/\lambda}\left(C_1e^{-\kappa' L}+C_2e^{\kappa' L}\right)-(C_1+C_2)\right\} + \phi_t\left\{n_{0s}\left(\gamma^{L/\lambda}-1\right) - n_{0d}\left(\gamma^{-L/\lambda}-1\right)\right\}\Big]$$

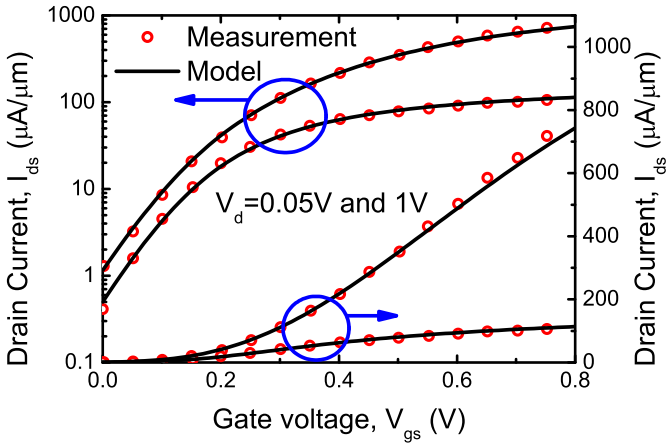

Fig. 2: Measurement and model results for drain current as a function of gate voltage for different drain biases. The measurement is for an $InGaAs$ device with $L = 20nm$, $W = 20nm$ and $EOT = 1.2nm$ ($0.5nm\ Al_2O_3 - 4nm\ LaAlO_3$ stack). [15].

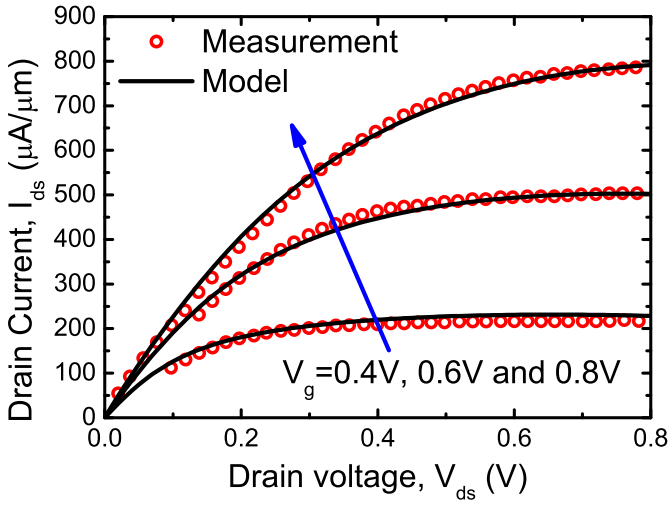

Fig. 3: Measured data along with prediction from the model for drain current as a function of the drain voltage for different gate voltages for the same device as in Fig. 2 [15]

components of the carrier density of the charges flowing from the drain to the source can be given as

$$n_{dd-drain}(x) = n_d\frac{S}{1-S}\gamma^{L-x/\lambda} = n_{0d}\gamma^{-x/\lambda};$$
$$n_{b-drain} = (1-S)^{L/\lambda}n_d \quad (5)$$

where $n_{0d} = n_d\frac{S}{1-S}\gamma^{L/\lambda}$ with n_d denoting the drain-side carrier density.

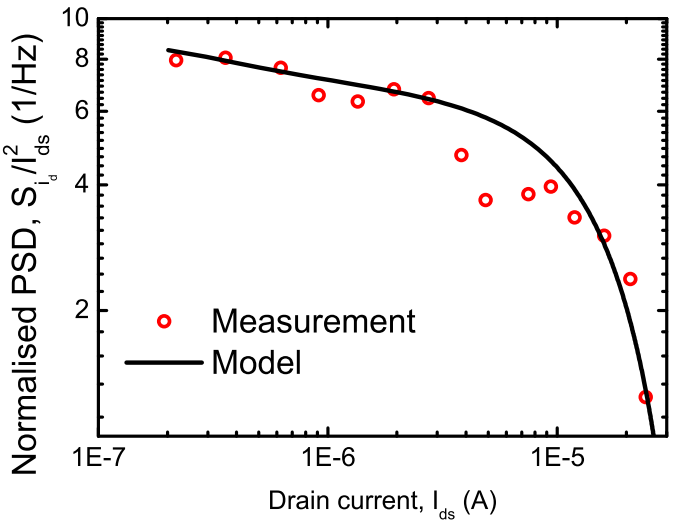

Fig. 4: Normalised noise PSD with varying drain current at $f = 10Hz$ and $V_{ds} = 0.05V$, as predicted by the model along with measured data for the same device as in Fig. 2 [15].

Eq (3) can used along with (4) and (5) to get the surface potential along the channel as (6) [17] where $\alpha = ln(\gamma)/\lambda$ and

$$M_1 = \frac{\kappa}{\alpha\xi}V_{gfb} - \frac{q\kappa}{\alpha\epsilon_s}n_{b-source} - \phi_t\alpha,$$
$$M_2 = \frac{q\kappa}{\alpha\epsilon_s}n_{b-drain} + \phi_t\alpha - \frac{\kappa}{\alpha\xi}V_{gfb},$$
$$N_{1,2} = \frac{q\kappa}{\alpha\epsilon_s}n_{0(s,d)},\ C_2 = \frac{K_2e^{\frac{\kappa L}{\alpha\xi}} - K_1}{e^{\frac{2\kappa L}{\alpha\xi}}-1},\ C_1 = K_1 - C2, \quad (7)$$
$$K_1 = \frac{\alpha\xi(M_2-M_1)}{\kappa} + \frac{N_2+N_1}{\alpha+\frac{\kappa}{\alpha\xi}} - (\kappa-1)V_{gfb},$$
$$K_2 = \kappa V_{ds} + \frac{\alpha\xi(M_2-M_1)}{\kappa} + \frac{N_2\gamma^{-L/\lambda}+N_1\gamma^{L/\lambda}}{\alpha+\frac{\kappa}{\alpha\xi}} - (\kappa-1)V_{gfb}$$

Using the surface potential and the carrier density, we can calculate the drain-to-source current as $I_{ds} = I_b + I_{dd}$, where I_b represents the ballistic component and I_{dd} represents the drift-diffusive component. I_b and I_{dd} are given as (8) and (9), respectively, where $\kappa' = \kappa/(\alpha\xi)$, A is the Fermi-Dirac

$$S_{i_d} = \frac{N_t kT}{N_{p_t} f^{EF}} \frac{P_1^2 N_1}{WL^2} \left[\frac{1}{2\alpha\sqrt{n_{0d}n_{0s}}} ln \left\{ \left(\frac{n_{0s}\gamma^{L/\lambda} - \sqrt{n_{0s}n_{0d}}}{n_{0s}\gamma^{L/\lambda} + \sqrt{n_{0s}n_{0d}}} \right) \left(\frac{n_{0s} + \sqrt{n_{0s}n_{0d}}}{n_{0s} - \sqrt{n_{0s}n_{0d}}} \right) \right\} + \frac{\Gamma_2}{\alpha} \left\{ n_{0s} \left(\gamma^{L/\lambda} - 1 \right) + n_{0d} \left(\gamma^{-L/\lambda} - 1 \right) \right\} \right. \tag{12}$$

$$\left. + \left(\Gamma_1 + \frac{N_2}{N_1}\Gamma_3 + \frac{N_3}{N_1} \right) L - \frac{N_2}{2\alpha\sqrt{n_{0d}n_{0s}}} ln \left\{ \left(\frac{n_{0s}\gamma^{L/\lambda} + \sqrt{n_{0s}n_{0d}}}{n_{0s}\gamma^{L/\lambda} - \sqrt{n_{0s}n_{0d}}} \right) \left(\frac{n_{0s} - \sqrt{n_{0s}n_{0d}}}{n_{0s} + \sqrt{n_{0s}n_{0d}}} \right) \right\} \right]$$

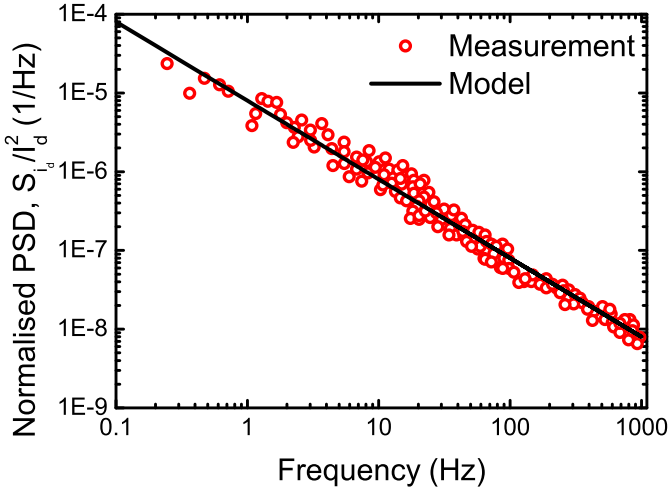

Fig. 5: Measurement and model results for normalised noise PSD as a function of frequency at $V_{ds} = V_{gs} = 0.05V$ for the same device as in Fig. 2. The linear decrease of the noise PSD with increasing frequency in the log-log scale is a signature of Flicker noise.

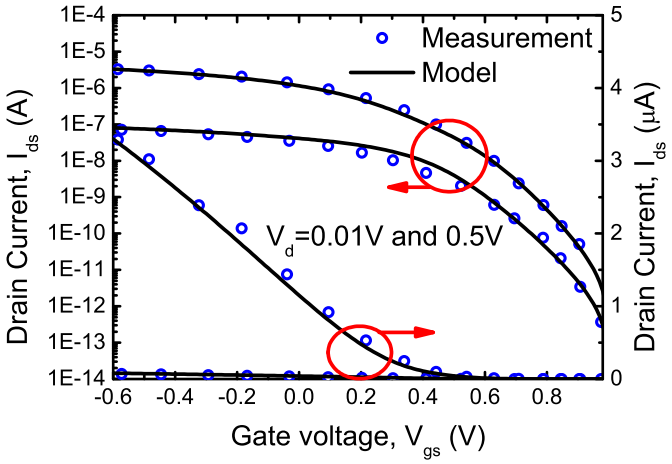

Fig. 6: Measurement and model results for the bais dependence of drain current for a Carbon nano-tube FET fabricated on heavily -doped Si substrate with Ti contacts. For this device, $L = 600nm$ and $EOT = 10nm$ [20], [21].

correction factor [2], L is the channel length and W is the effective channel width. The ballistic velocity, v_b, is calculated as in [2] and the short channel effects are taken into account as described in [2], [19].

III. Flicker Noise Model

It is widely accepted that Flicker noise is caused due to the trapping/de-trapping of charge carriers. The change in the drain current due to trapping/de-trapping of charges can be

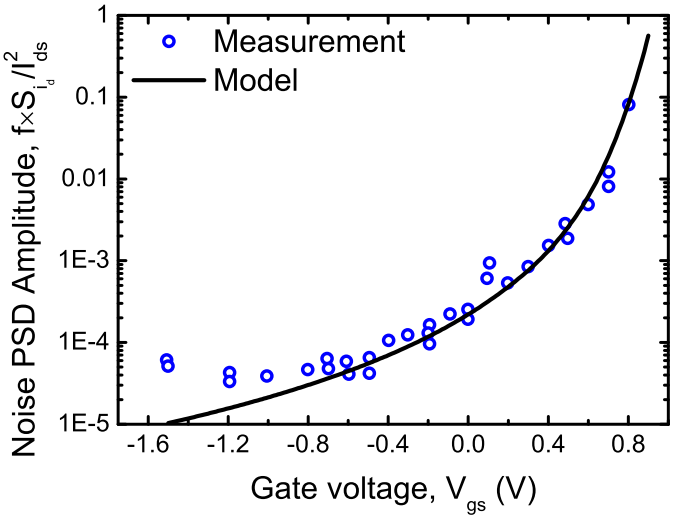

Fig. 7: Noise PSD amplitude, fS_{i_d}/I_{ds}^2, as function of the gate voltage at $V_{ds} = 0.01V$, as obtained through model simulations and experimental measurements of the same device as in Fig. 6 [20].

given as

$$\frac{\partial I_{ds}}{\partial N_t} = P_1 \left(P_2 \frac{\partial I_{dd}}{\partial N_t} + \frac{\partial I_b}{\partial N_t} \right)$$

$$\frac{\partial I_{ds}}{\partial N_t} = P_1 \left(P_2 I_{dd} \left[\frac{1}{\mu} \frac{d\mu}{dN_t} + \frac{1}{n_{dd}} \underbrace{\frac{dn_{dd}}{dN_t}}_{R_{Nd}} \right] + \frac{I_b}{n_b} \underbrace{\frac{dn_b}{dN_t}}_{R_{Nb}} \right) \tag{10}$$

where N_t denotes the vacant trap concentration and P_1 and P_2 are coefficients dependent on channel length modulation and velocity saturation respectively [16]. The drain current noise PSD, S_{i_d}, can be calculated as

$$S_{i_d} = \frac{S_N}{WL^2} \int_0^L \left(\frac{\partial I_{ds}}{\partial N_t} \right)^2 dx \tag{11}$$

where $S_N = qN_t\phi_t/(N_{P_t} f^{EF})$. N_{P_t} depends on the probability of tunneling of charge carriers to/from the trapping sites, $n_{dd} = n_{dd-source} - n_{dd-drain}$, $n_b = n_{b-source}(x = L) - n_{b-drain}(x = 0)$, f denotes the frequency of operation and EF is a parameter. The final analytical expression for S_{i_d} is given as (12), where $N_1 = (P_2 I_{dd})^2$, $N_2 = I_b I_{dd} P_2/n_b$, $N_3 = (I_b/n_b)^2$ and Γ_1, Γ_2 and Γ_3 are parameters.

IV. Results and Discussion

The model is validated with electrical measurements of an $InGaAs$ nanowire FET [15] and a Carbon Nanotube FET [20]. Both the devices are operating in the quasi-ballistic

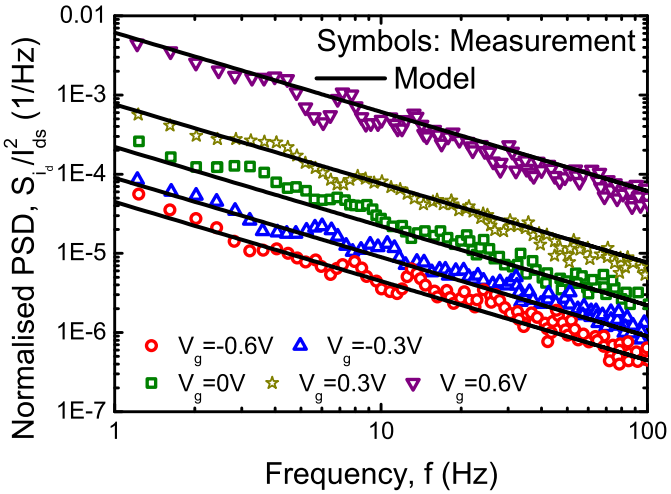

Fig. 8: Measurement and model results for frequency and bias dependence of the normalised noise PSD at $V_{ds} = 0.01V$, for the same device as in Fig. 6 [20].

regime [15], [20]. The DC model parameters are extracted based on an accurate match with the DC current-voltage data. Using this set of parameters, the model is then validated with noise measurements using only the noise parameters γ_1, γ_2 and γ_3.

Fig. 2 and Fig. 3 show the measured data of the drain current along with the prediction by the model, as a function of the gate voltage and drain voltage, respectively, for the InGaAs nanowire FET [15]. As can be seen, the model is able to capture the DC current behaviour accurately. Fig. 4 shows the bias dependence of the normalised noise power spectral density (PSD) while Fig. 5 shows the frequency dependence. Fig. 5 clearly shows the $\frac{1}{f}$ behaviour of the noise PSD, which is a trademark of flicker noise.

Fig. 6 shows the measurement and the model prediction for the drain current as a function of different gate and drain biases. Fig. 7 shows the noise PSD amplitude, defined as fS_{i_d}/I_{ds}^2, with varying gate voltage and Fig. 8 shows the frequency dependence of the normalised noise PSD for different gate biases. The model results are able to match all the measurements with good accuracy.

V. Conclusion

We have presented a model for Flicker noise in quasi-ballistic systems. This model is an improvement over the existing model [16] brought about by the improved core model for transport in quasi-ballistic systems [17]. The model has been validated with experimental measurements and shows good agreement.

Acknowledgement

This work is funded by the Department of Science and Technology (DST), Govt. of India; and the Council of Scientific and Industrial Research (CSIR), Govt. of India.

References

[1] K. Natori, "Ballistic/quasi-ballistic transport in nanoscale transistor", *Applied Surface Science*, vol. 254, no. 19, pp. 6194-6198, 2008.

[2] A. Dasgupta, A. Agarwal, S. Khandelwal and Y. S. Chauhan, "Compact Modeling of Surface Potential, Charge, and Current in Nanoscale Transistors Under Quasi-Ballistic Regime", *IEEE Transactions on Electron Devices*, vol. 63, no. 11, pp. 4151-4159, 2016.

[3] A. Rahman and M. Lundstrom, "A compact scattering model for the nanoscale double-gate MOSFET", *IEEE Transactions on Electron Devices*, vol. 49, no. 3, pp. 481-489, 2002.

[4] S. Martinie, D. Munteanu, G. L. Carval, and J.-L. Autran, "Physics-based analytical modeling of quasi-ballistic transport in double-gate MOSFETs: From device to circuit operation", *IEEE Transactions on Electron Devices*, vol. 56, no. 11, pp. 26922702, 2009.

[5] L. Wei, O. Mysore, and D. Antoniadis, "Virtual-source-based self-consistent current and charge FET models: From ballistic to drift-diffusion velocity-saturation operation", *IEEE Transactions on Electron Devices*, vol. 59, no. 5, pp. 1263-1271, 2012.

[6] M.-J. Chen and L.-F. Lu, "A parabolic potential barrier-oriented compact model for the kB T layers width in nano-MOSFETs", *IEEE Transactions on Electron Devices*, vol. 55, no. 5, pp. 1265-1268, 2008.

[7] A. Mangla, J.-M. Sallese, C. Sampedro, F. Gamiz, and C. Enz, "Modeling the Channel Charge and Potential in Quasi-Ballistic Nanoscale Double-Gate MOSFETs", *IEEE Transactions on Electron Devices*, vol. 61, no. 8, pp. 2640-2646, 2014.

[8] H. Wang and G. Gildenblat, "Scattering matrix based compact MOSFET model", *IEEE International Electron Devices Meeting*, pp. 125-128, 2002.

[9] S. Khandelwal, H. Agarwal, P. Kushwaha, J. P. Duarte, A. Medury, Y. S. Chauhan, S. Salahuddin and C. Hu, "Unified Compact Model Covering Drift-Diffusion to Ballistic Carrier Transport", *IEEE Electron Device Letters*. vol. 37, no. 2, pp. 134-137, 2016.

[10] M. S. Lundstrom and D. A. Antoniadis, "Compact Models and the Physics of Nanoscale FETs", *IEEE Transactions on Electron Devices*, vol. 61, no. 2, pp. 225-233, 2014.

[11] G. Mugnaini and G. Iannaccone, "Physics-based compact model of nanoscale MOSFETsPart I: Transition from drift-diffusion to ballistic transport", *IEEE Transactions on Electron Devices*, vol. 52, no. 8, pp. 1795-1801, 2005.

[12] G. Mugnaini and G. Iannaccone, "Physics-based compact model of nanoscale MOSFETsPart II: Effects of degeneracy on transport", *IEEE Transactions Electron Devices*, vol. 52, no. 8, pp. 1802-1806, 2005.

[13] S. Rakheja, M. S. Lundstrom and D. A. Antoniadis, "An Improved Virtual-Source-Based Transport Model for Quasi-Ballistic TransistorsPart I: Capturing Effects of Carrier Degeneracy, Drain-Bias Dependence of Gate Capacitance, and Nonlinear Channel-Access Resistance", *IEEE Transactions on Electron Devices*, vol. 62, no. 9, pp. 2786-2793, 2015.

[14] S. Rakheja, M. S. Lundstrom and D. A. Antoniadis, "An Improved Virtual-Source-Based Transport Model for Quasi-Ballistic TransistorsPart II: Experimental Verification", *IEEE Transactions on Electron Devices*, vol. 62, no. 9, pp. 2794-2801, 2015.

[15] N. Conrad, M. Si, S. H. Shin, J. J. Gu, J. Zhang, M. A. Alam and P. D. Ye, "Low-Frequency Noise and RTN on Near-Ballistic III-V GAA Nanowire MOSFETs", *IEEE International Electron Devices Meeting*, pp. 20.1.1-20.1.4, 2014.

[16] A. Dasgupta, H. Agarwal, A. Agarwal and Y. S. Chauhan, "Modeling of Flicker Noise in Quasi-ballistic devices", *IEEE International Conference on Emerging Electronics (ICEE)*, 2016.

[17] A. Dasgupta, A. Agarwal and Y. S. Chauhan, "An Improved Model for Quasi-Ballistic Transport in MOSFETs", in *IEEE Transactions on Electron Devices* , vol.PP, no.99, pp.1-5, 2017.

[18] S. Khandelwal, Y. S. Chauhan and T. A. Fjeldy, "Analytical modeling of Surface-Potential and intrinsic charges in AlGaN/GaN HEMT devices", *IEEE Transactions on Electron Devices*, vol. 59, no. 10, pp. 2856-2860, 2012.

[19] Y. S. Chauhan, D. Lu, S. Venugopalan, S. Khandelwal, J. P. Duarte, N. Paydavosi, A. M. Niknejad, and C. Hu , "FinFET Modeling for IC Simulation and Design: Using the BSIM-CMG Standard", *Academic Press*, 2015.

[20] Y.-M. Lin, J. Appenzeller, J. Knoch, Z. Chen and P. Avouris, "Low-Frequency Current Fluctuations in Individual Semiconducting Single-Wall Carbon Nanotubes", *Nano Letters*, vol. 6, no. 5, pp. 930-936, 2006.

[21] Y.-M. Lin, J. Appenzeller, J. Knoch, and P. Avouris, "High-Performance Carbon Nanotube Field-Effect Transistor With Tunable Polarities", *IEEE Transactions on Nanotechnology*, vol. 4, no. 5, pp. 481-489, 2005.